In conclusion, we have demonstrated the value of immunoassays for the development of highly efficient methods to screen enantioselective catalysts. The underlying principle of the procedure is general and should be successfully applied to any type of catalysis if one has antibodies with the required binding specificity. In fact, the immune system itself is a huge combinatorial machine providing a diverse set of specific binding molecules, and it is generally accepted that antibodies can be raised against virtually any compound of interest according to one's need. Furthermore, the use of antibodies for automated assays is routine and involves simple and time-saving experimental procedures. For these reasons, immunoassays appear to be effective ways of developing new high-throughput screening for the discovery of catalysts.

Received: September 17, 2001 [Z17920]

[1] a) W. F. Maier, *Angew. Chem.* **1999**, *111*, 1294 – 1296; *Angew. Chem. Int. Ed.* **1999**, *38*, 1216 – 1223; b) B. Jandeleit, D. J. Shaefer, T. S. Powers, H. W. Turner, W. H. Weinberg, *Angew. Chem.* **1999**, *111*, 2648 – 2689; *Angew. Chem. Int. Ed.* **1999**, *38*, 2494 – 2532; c) K. D. Shimizu, M. L. Snapper, A. H. Hoveyda, *Chem. Eur. J.* **1998**, *4*, 1885 – 1889.

[2] a) O. Lavastre, J. P. Morken, *Angew. Chem.* **1999**, *111*, 3357 – 3359; *Angew. Chem. Int. Ed.* **1999**, *38*, 3163 – 3165; b) C. Hinderling, P. Chen, *Angew. Chem. Int. Ed.* **1999**, *38*, 2253 – 2256; c) K. Mikami, R. Angelaud, K. Ding, A. Ishii, A. Tanaka, N. Sawada, K. Kudo, M. Senda, *Chem. Eur. J.* **2001**, *7*, 730 – 737; d) K. Ding, A. Ishii, K. Mikami, *Angew. Chem.* **1999**, *111*, 519 – 523; *Angew. Chem. Int. Ed.* **1999**, *38*, 497 – 501; e) R. H. Crabtree, *Chem. Commun* **1999**, 1611 – 1616; f) K. H. Shaughnessy, P. Kim, J. F. Hartwig, *J. Am. Chem. Soc.* **1999**, *121*, 2123 – 2132; g) A. C. Cooper, L. H. McAlexander, D. H. Lee, M. T. Torres, R. H. Crabtree, *J. Am. Chem. Soc.* **1998**, *120*, 9971 – 9972; h) A. M. Porte, J. Reibenspies, K. Burgess, *J. Am. Chem. Soc.* **1998**, *120*, 9180 – 9187; i) M. S. Sigman, E. N. Jacobsen, *J. Am. Chem. Soc.* **1998**, *120*, 4901 – 4902; j) K. D. Shimizu, B. M. Cole, C. A. Krueger, K. W. Kuntz, M. L. Snapper, A. H. Hoveyda, *Angew. Chem.* **1997**, *109*, 1781 – 1785; *Angew. Chem. Int. Ed. Engl.* **1997**, *36*, 1704 – 1707; k) K. Burgess, H. J. Lim, A. M. Porte, G. A. Sulikowski, *Angew. Chem.* **1996**, *108*, 192 – 194; *Angew. Chem. Int. Ed. Engl.* **1996**, *35*, 220 – 222.

[3] a) L. E. Janes, R. J. Kazlauskas, *J. Org. Chem.* **1997**, *62*, 4560 – 4561; b) L. E. Janes, A. C. Löwendahl, R. J. Kazlauskas, *Chem. Eur. J.* **1998**, *4*, 2324 – 2331.

[4] a) G. T. Copeland, S. J. Miller, *J. Am. Chem. Soc.* **1999**, *121*, 4306 – 4307; b) M. B. Francis, E. N. Jacobsen, *Angew. Chem.* **1999**, *111*, 987 – 991; *Angew. Chem. Int. Ed. Engl.* **1999**, *38*, 937 – 941.

[5] a) S. J. Taylor, J. P. Morken, *Science* **1998**, *280*, 267 – 270; b) M. T. Reetz, M. H. Becker, K. M. Kühling, A. Holtzwarth, *Angew. Chem.* **1998**, *110*, 2792 – 2795; *Angew. Chem. Int. Ed. Engl.* **1998**, *37*, 2647 – 2650.

[6] M. T. Reetz, K. M. Kühling, A. D. Deege, H. Hinrichs, D. Belder, *Angew. Chem.* **2000**, *112*, 4049 – 4052; *Angew. Chem. Int. Ed. Engl.* **2000**, *39*, 3891 – 3893.

[7] M. T. Reetz, M. H. Becker, H. W. Klein, D. Stöckigt, *Angew. Chem.* **1999**, *111*, 1872 – 1875; *Angew. Chem. Int. Ed. Engl.* **1999**, *38*, 1758 – 1761.

[8] For recent reviews on *ee* assays see: a) M. T. Reetz, *Angew. Chem.* **2001**, *113*, 292 – 320; *Angew. Chem. Int. Ed. Engl.* **2001**, *40*, 284 – 310; b) T. J. Edkins, D. R. Bobbitt, *Anal. Chem.* **2001**, *93*, 488A – 496A.

[9] a) X. F. Duan, C. L. Yin, *Synth. Commun.* **1997**, *27*, 825 – 828; b) E. J. Corey, J. O. Link, Y. Shao *Tetrahedron. Lett.* **1992**, *33*, 3435 – 3438; c) D. A. Evans, M. M. Morrissey, R. L. Dorow, *J. Am. Chem. Soc.* **1985**, *107*, 4346 – 4348.

[10] a) Z. Wang, B. La, J. M. Fortunak, *Tetrahedron Lett.* **1998**, *39*, 5501 – 5504; b) F. M. Menger, C. A. West, J. Ding, *Chem. Commun.* **1997**, 633 – 634; c) A. Schummer, H. Yu, H. Simon, *Tetrahedron* **1991**, *47*, 9019 – 9034.

[11] F. Taran, P. Y. Renard, C. Créminon, A. Valleix, Y. Frobert, P. Pradelles, J. Grassi, C. Mioskowski, *Tetrahedron Lett.* **1999**, *40*, 1891 – 1894.

[12] O. Hofstetter, H. Hofstetter, M. Wilchek, V. Schurig, B. S. Green, *J. Am. Chem. Soc* **1998**, *120*, 3251 – 3252.

[13] O. Hofstetter, H. Hofstetter, M. Wilchek, V. Schurig, B. S. Green, *Chem. Commun.* **2000**, 1581 – 1582; O. Hofstetter, H. Hofstetter, M. Wilchek, V. Schurig, B. S. Green, *Nat. Biotechnol.* **1999**, *17*, 371 – 374.

[14] F. Taran, P. Y. Renard, H. Bernard, C. Mioskowski, Y. Frobert, P. Pradelles, J. Grassi, *J. Am. Chem. Soc.* **1998**, *120*, 3332 – 3339.

Ordered Langmuir – Blodgett Films of Amphiphilic β-Hairpin Peptides Imaged by Atomic Force Microscopy**

Evan T. Powers, Sung Ik Yang, Charles M. Lieber,* and Jeffery W. Kelly*

Langmuir and Langmuir – Blodgett (LB) films of peptides have a number of potential applications.[1–7] The fulfillment of this potential will depend on developing the molecular level understanding needed to control both the order within these films and their structures. Self-assembly in thin peptide films can be characterized by circular dichroism[8–10] and IR[11, 12] spectroscopies, fluorescence microscopy,[13–15] and at high resolution by grazing incidence X-ray diffraction (GIXD),[3, 14] and atomic force microscopy (AFM).[5, 16] Previous fluorescence microscopy results demonstrate that peptide **1** self-assembles into liquid- and solid-phase domains at the air – water (A – W) interface.[13] Here, we have used AFM with carbon nanotube tips to image LB films of **1** and its longer relative, **2**. The images show crystalline, two-dimensional order in films of **1** and **2** and demonstrate that the assembly parameters can be varied through well-defined changes in peptide structure.

The 14- and 18-residue peptides **1** and **2** both have a DPro-Gly sequence in the middle of alternating hydrophilic (Glu)

[*] Prof. C. M. Lieber, Dr. S. I. Yang[+]
Department of Chemistry and Chemical Biology
Harvard University
Cambridge, MA 02138 (USA)
Fax: (+1) 617-496-5442
E-mail: cml@cmliris.harvard.edu

Prof. J. W. Kelly, Prof. E. T. Powers[+]
Department of Chemistry and The Skaggs Institute of Chemical Biology
The Scripps Research Institute
La Jolla, CA 92037 (USA)
Fax: (+1) 858-784-9610
E-mail: jkelly@scripps.edu

[+] E. T. Powers and S. I. Yang contributed equally to this work.

[**] This work was supported by the NIH (GM 51105), the Skaggs Institute of Chemical Biology, the Lita Annenberg Hazen Foundation, and the Air Force Office of Scientific Research. E. T. P. thanks the NIH for an NRSA.

Supporting information for this article is available on the WWW under http://www.angewandte.com or from the author.

Gly–Val–Glu–Nle–Glu–Nle–Glu–NH_2
|
DPro–Val–Glu–Nle–Glu–Cys (DMBDY)–Glu–H **1**

Gly–Val–Glu–Nle–Glu–Nle–Glu–Nle–Glu–NH_2
|
DPro–Val–Glu–Nle–Glu–Nle–Glu–Cys (DMBDY)–Glu–H **2**

and hydrophobic (Val, norleucine (Nle), labeled Cys) residues. The DPro-Gly sequence favors type II′ β-turn conformations,[17, 18] while alternating hydrophilic/hydrophobic sequences at the A – W interface favor β-strand conformations,[2, 9, 19] making it likely that **1** and **2** will form amphiphilic β-hairpins at the A – W interface. The sole cysteines in **1** and **2** were labeled with the 5,7-dimethyl derivative of the BODIPY (Molecular Probes) fluorophore (DMBDY) for concentration determination.[13]

The surface pressure – molecular area (Π-A) isotherms in Figure 1 show that monolayers of **1** and **2** spread on deionized water (DIW) are stable although about 20% of **1** dissolves after spreading, consistent with its known water solubility.[13] The Π-A isotherm of **1** has been corrected to account for this

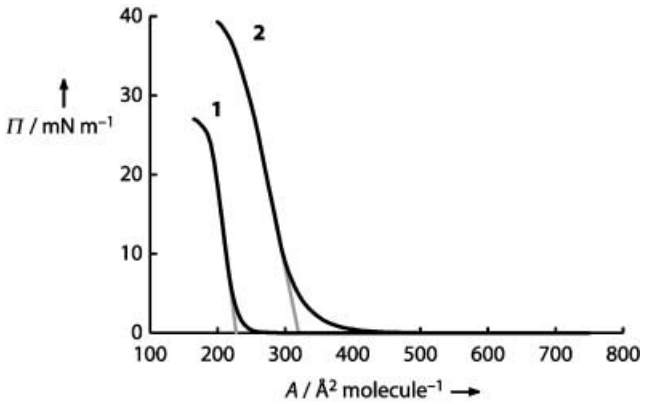

Figure 1. Black lines: Surface pressure – molecular area (Π-A) isotherms for **1** and **2** on DIW. Gray lines: extrapolations to the x axis from the points of steepest slope on the isotherms.

(see Supporting Information for details). Peptide **2** dissolves to a much lesser extent, so its Π-A isotherm is not corrected. The limiting molecular areas of **1** and **2**, obtained by extrapolation of the Π-A isotherm to the x axis,[20] are 230 Å^2 molecule^{-1} for **1** and 320 Å^2 molecule^{-1} for **2**.

Single layer LB films of **1** and **2** were deposited at 10 mN m^{-1} onto freshly cleaved mica (with the hydrophilic side of the monolayer facing the substrate and the hydrophobic side facing outward). The LB monolayers were then imaged by tapping mode AFM using single-wall carbon nanotube (SWNT) tips. SWNT tips have many advantages over Si tips, the most important here being reproducibly high lateral resolution.[21] This resolution is evident in Figure 2 and

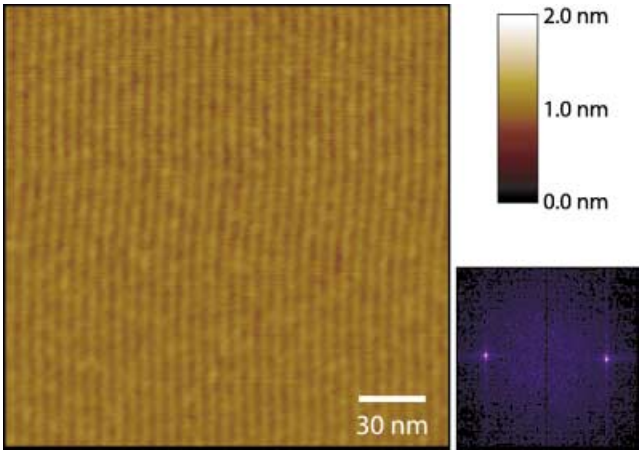

Figure 2. Left: AFM image of an LB monolayer of **1** deposited at 10 mN m^{-1} on mica. Right: height scale and Fourier transform of the image.

3, which show representative images of LB monolayers of **1** and **2**, respectively. Patterns of ridges with peak-to-trough heights of 2 – 4 Å are prominent in both Figure 2 and 3. Although similar features can be observed by using standard microfabricated tips, the SWNT tips enable lattice-resolved data to be obtained reproducibly without the need to search for a "good" tip. The repeat periods of the ridges can be determined from the images' Fourier transforms (FT). There

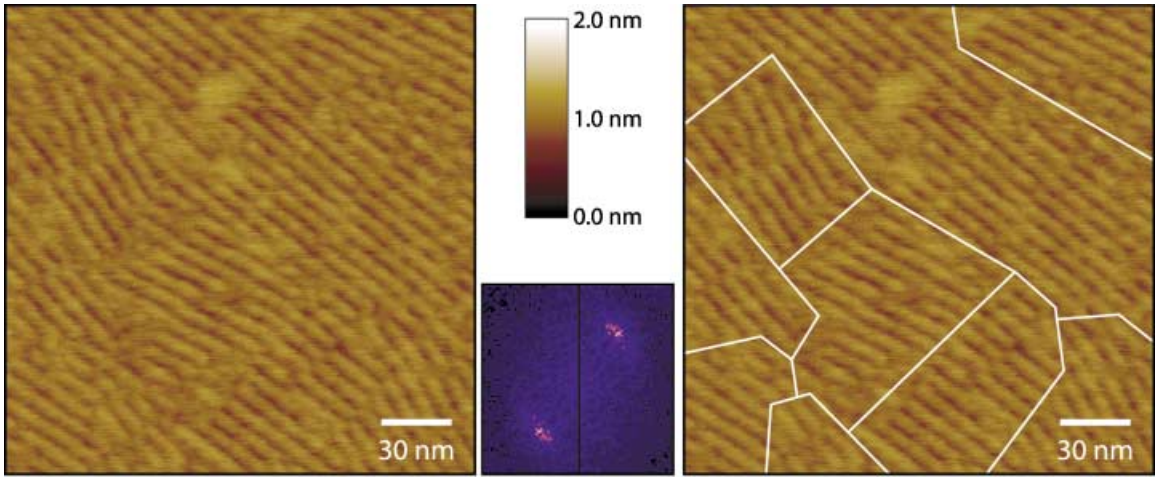

Figure 3. Left: AFM image of an LB monolayer of **2** deposited at 10 mN m^{-1} on mica. Middle: height scale and Fourier transform of the image. Right: Scan area divided into domains.

  1433-7851/02/4101-0128 $ 17.50+.50/0 *Angew. Chem. Int. Ed.* **2002**, *41*, No. 1

is only one set of parallel ridges in Figure 2, corresponding to a single maximum in the FT at 61 Å. In contrast, there are several domains of parallel ridges in Figure 3, corresponding to a radial streak in the FT at around 74 Å. The average ridge periods obtained from over 70 measurements each on LB monolayers of **1** and **2** are similar to those found above: 59(±1) Å for **1** and 74(±1) Å for **2**. The monolayer height, measured from holes in the films to the tops of the ridges, is 7(±1) Å.

Figure 2 vividly illustrates the crystallinity in monolayers of **1**. Here, a single domain extends for hundreds of nanometers in the directions parallel and perpendicular to the ridges. Images from larger scan areas (see Supporting Information) show that such domain sizes are typical for **1**, attesting to its strong propensity to assemble. The use of 1–2 nm diameter tips provides high confidence that defects are not being averaged out by the use of large contact area tips, and that the region shown is indeed virtually defect-free. Although defects such as grain boundaries appear in other images, LB monolayers of **1** are generally very well ordered.

Figure 3 demonstrates that the ridge period can be increased (from 59 Å to 74 Å) by adding residues to the peptide, while retaining a great deal of order in the monolayer. Although the domains outlined in Figure 3 are smaller than the one in Figure 2, they still persist for tens of nanometers. Images from larger scan areas (see Supporting Information) show that such sizes are typical. The effects on the assembly of the added residues in **2** (increased ridge period and decreased domain sizes) mirror the observations of Rapaport and coworkers on peptide monolayers at the A–W interface.[3] They also found that the lattice spacing increased and monolayer order decreased with increasing peptide length. This correspondence suggests that a monolayer's state at the A–W interface directly influences the degree of order in LB films.

The features in these LB monolayers can only be fruitfully discussed in light of a structural model. Such a model for **1**, based on the high β-sheet content found previously in its LB monolayers[13] and the AFM images above, is illustrated in Figure 4. The assembly consists of β-hairpins of **1**, each 9.4 Å wide and 25 Å long (according to typical β-sheet dimensions[22]). These associate by hydrogen bonding in the direction perpendicular to the strands to form cross-β sheets. These sheets have two interfaces: a polar one composed of the termini and a nonpolar one composed of the turns. They are assembled laterally along both interfaces, driven by electrostatic and van der Waals interactions, respectively. The expected monolayer height in this model is 7–10 Å depending on the side chain conformations, matching the observed height of 7 Å. Individual ridges correspond to pairs of cross-β sheets assembled along their polar interfaces, making the expected ridge period 55 Å. This is within 7% of the observed (59 Å) ridge period.

The model is supported by the match between the expected and observed ridge periods, but its further evaluation is complicated by the AFM images' providing only one lattice parameter, the ridge period, when three are required to define a two-dimensional unit cell. Other information can, however, be used to judge the model. For example, we note that by

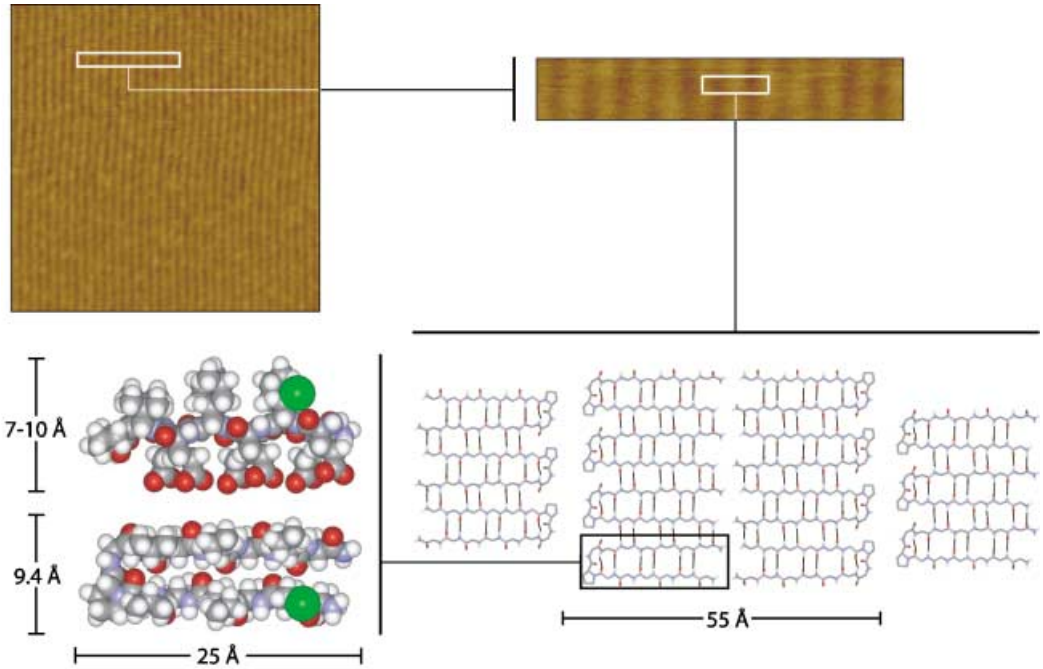

Figure 4. Molecular model for the assembly of **1**. The scan area from Figure 2 is shown in the top left. A white box encloses a small section of the scan area, which is expanded in the top right. Another white box in the expansion encloses a ridge with two flanking half-ridges. A molecular model for the assembly in the enclosed area is shown in the bottom right. The central ridge corresponds to the two central columns of β-hairpins, which interact with each other through their polar termini. The flanking half-ridges correspond to the two flanking columns of β-hairpins, which interact with the central column through turn-turn recognition. The ridge period expected from this model is 55 Å: 25.0 Å for each hairpin, 2 Å for the gap at the termini-to-termini interface (a typical distance for hydrogen bonds[26]), and 3 Å for the gap at the turn-to-turn interface (a typical distance for van der Waals interactions[27]). The panel in the bottom left shows a top view (lower part of panel) and a side view (upper part) of a single hairpin. The hairpin's length is 25 Å and its width is 9.4 Å (see top view), while its height can be from 7 to 10 Å depending on the side chains' conformations (see side view). The green spheres represent the DMBDY fluorophore.

  1433-7851/02/4101-0129 $ 17.50+.50/0

having the D-prolines in the turns rather than in the strands, the model accounts for proline's strong propensity to break β-sheet structure.[3, 23, 24] The model is also consistent with the molecular areas determined from the Π-A isotherms. The molecular areas based on the hairpin dimensions and the measured ridge periods are 9.4 Å × ½ × 59 Å = 277 Å^2 for **1** and 9.4 Å × ½ × 74 Å = 348 Å^2 for **2**. These are within 18% and 9% of their experimentally determined values (230 Å^2 and 320 Å^2). Finally, the model accounts for how peptide length can be used to control the ridge period. Because the strands are perpendicular to the ridges, **2** should produce ridge periods 13.8 Å longer than those of **1** since it is four residues longer (4 × 3.45 Å). This is within 8% of the observed difference.

In summary, AFM images obtained using single-wall carbon nanotube tips show that LB monolayers of **1** and **2** are organized into two-dimensional domains of laterally assembled cross-β sheets. These sheets appear as ridges in the AFM images. Individual domains extend for hundreds of nanometers in LB monolayers of **1** and tens of nanometers in LB monolayers of **2**. Finally, the size of the ridges can be directly controlled through the peptide length.

Experimental Section

The preparation of **1** has been described elsewhere.[13] Peptide **2** was prepared by the same method and characterized by electrospray ionization mass spectrometry (M^- = 2360.7, expected: 2360.3). Peptides were spread from solutions in 1:1 DIW:ethanol. Isotherms were measured 30 min after spreading on DIW at room temperature on a Nima 611 LB Trough with a compression rate of 5 cm^2 min^{-1}. See Supporting Information for details of peptide concentration determination in the spreading solutions and subphase. LB films were deposited using a KSV 5000 LB trough by rapidly compressing monolayers to 10 mN m^{-1}, holding for 10 min, then lifting freshly cleaved mica substrates through the surface at 2 mm min^{-1}. AFM measurements were made in air using a Digital Instruments Multimode Nanoscope IIIa in Tapping Mode. SWNT tips were prepared as described previously.[25]

Received: September 27, 2001 [Z17983]

[1] H. Bekele, J. H. Fendler, J. W. Kelly, *J. Am. Chem. Soc.* **1999**, *121*, 7266 – 7267.
[2] M. Boncheva, H. Vogel, *Biophys. J.* **1997**, *73*, 1056 – 1072.
[3] H. Rapaport, K. Kjaer, T. R. Jensen, L. Leiserowitz, D. A. Tirrell, *J. Am. Chem. Soc.* **2000**, *122*, 12523 – 12529.
[4] C. Steinem, A. Janshoff, M. S. Vollmer, M. R. Ghadiri, *Langmuir* **1999**, *15*, 3956 – 3964.
[5] A. L. Weisenhorn, D. U. Romer, G. P. Lorenzi, *Langmuir* **1992**, *8*, 3145 – 3149.
[6] G. Xu, W. Wang, J. T. Groves, M. H. Hecht, *Proc. Natl. Acad. Sci. USA* **2001**, *98*, 3652 – 3657.
[7] K. Fujita, S. Kimura, Y. Imanishi, E. Rump, H. Ringsdorf, *J. Am. Chem. Soc.* **1994**, *116*, 2185 – 2186.
[8] D. G. Cornell, *J. Colloid Interface Sci.* **1979**, *70*, 167 – 180.
[9] W. F. DeGrado, J. D. Lear, *J. Am. Chem. Soc.* **1985**, *107*, 7684 – 7689.
[10] J. W. Taylor, *Biochemistry* **1990**, *29*, 5364 – 5373.
[11] D. Blaudez, T. Buffeteau, B. Desbat, J. M. Turlet, *Curr. Opin. Colloid Interface Sci.* **1999**, *4*, 265 – 272.
[12] R. Mendelsohn, J. W. Brauner, A. Gericke, *Annu. Rev. Phys. Chem.* **1995**, *46*, 305 – 334.
[13] E. T. Powers, J. W. Kelly, *J. Am. Chem. Soc.* **2001**, *123*, 775 – 776.
[14] R. Ionov, A. El-Abed, A. Angelova, M. Goldmann, P. Peretti, *Biophys. J.* **2000**, *78*, 3026 – 3035.
[15] K. Fujita, S. Kimura, Y. Imanishi, E. Rump, H. Ringsdorf, *Langmuir* **1995**, *11*, 253 – 258.
[16] S. E. Taylor, B. Desbat, D. Blaudez, S. Jacobi, L. F. Chi, H. Fuchs, G. Schwarz, *Biophys. Chem.* **2000**, *87*, 63 – 72.
[17] I. L. Karle, S. K. Awasthi, P. Balaram, *Proc. Natl. Acad. Sci. USA* **1996**, *93*, 8189 – 8193.
[18] H. E. Stanger, S. H. Gellman, *J. Am. Chem. Soc.* **1998**, *120*, 4236 – 4237.
[19] R. Maget-Dana, D. Lelievre, A. Brack, *Biopolymers* **1999**, *49*, 415 – 423.
[20] R. Maget-Dana, *Biochim. Biophys. Acta* **1999**, *1462*, 109 – 140.
[21] S. S. Wong, J. D. Harper, P. T. Lansbury, C. M. Lieber, *J. Am. Chem. Soc.* **1998**, *120*, 603 – 604.
[22] R. D. B. Fraser, T. P. MacRae, *Conformation in Fibrous Proteins and Related Synthetic Polypeptides*, Academic Press, London, **1973**.
[23] D. L. Minor, Jr., P. S. Kim, *Nature* **1994**, *367*, 660 – 663.
[24] S. J. Wood, R. Wetzel, J. D. Martin, M. R. Hurle, *Biochemistry* **1995**, *34*, 724 – 730.
[25] J. H. Hafner, C.-L. Cheung, T. H. Oosterkamp, C. M. Lieber, *J. Phys. Chem. B* **2001**, *105*, 743 – 746.
[26] G. A. Jeffrey, W. Saenger, *Hydrogen Bonding in Biological Structures*, Springer, Berlin, **1991**.
[27] J. N. Israelachvili, *Intermolecular and Surface Forces*, Academic Press, London, **1991**.

An Unprecedented Mixed-Charged State in a Supramolecular Assembly of Ligand-Based Mixed-Valence Redox Isomers $(ET^{\bullet+})_3[Cr^{III}(Cl_4SQ)_2(Cl_4Cat)]^-[Cr^{III}(Cl_4SQ)(Cl_4Cat)_2]^{2-}$**

Ho-Chol Chang and Susumu Kitagawa*

A metal complex containing noninnocent ligands serves as a useful module for synthesizing functional supramolecular assemblies whose physical and/or chemical properties are based on charges and spins. This is exemplified by the family of homoleptic *o*-quinone complexes, which provides unique charged and spin states irrespective of their simple constituent, $C_6O_2X_4$ (X = H or a halogen atom).[1] The freedom of their electronic states, for instance, is related to the redox forms of the ligand; *o*-benzoquinone, (BQ), *o*-semiquinonate (SQ), and catecholate (Cat). We have focused our interest on the ligand-based mixed-valence (LBMV) state of the ligands,

[*] Prof. S. Kitagawa, Dr. H.-C. Chang
Department of Synthetic Chemistry and Biological Chemistry Graduate School of Engineering, Kyoto University
Yoshida, Sakyo-ku, Kyoto 606-8501 (Japan)
Fax: (+81) 75-753-4979
E-mail: kitagawa@sbchem.kyoto-u.ac.jp

[**] This work was supported by a Grant-in-Aid for Scientific Research (Priority Area No. 10149101) from The Ministry of Education, Culture, Sports, Science, and Technology of Japan. We thank Dr. Hiroyuki Nishikawa (Tokyo Metropolitan University) for the electric conductivity measurements, and Prof. Tadaoki Mitani and Dr. Takashi Okubo (Japan Advanced Institute of Science and Technology) for their support regarding the Raman spectroscopic measurements. ET = bis(ethylenedithio)tetrathiafulvalene, SQ = *o*-semiquinonate, Cat = catecholate.

Supporting information for this article is available on the WWW under http://www.angewandte.com or from the author.

  1433-7851/02/4101-0130 $ 17.50+.50/0